Analyses of Ca^{2+} Accumulation and Dynamics in the Endoplasmic Reticulum of Arabidopsis Root Cells Using a Genetically Encoded Cameleon Sensor[1][C][W]

Maria Cristina Bonza[2], Giovanna Loro[2], Smrutisanjita Behera, Andrea Wong, Jörg Kudla, and Alex Costa*

Department of Biosciences, University of Milan, 20133 Milan, Italy (M.C.B., G.L., A.C.); Department of Biology (G.L.) and Department of Biomedical Sciences (A.W.), University of Padua, 35131 Padova, Italy; Institut für Biologie und Biotechnologie der Pflanzen, Universität Münster, 48149 Münster, Germany (S.B., J.K.); and Institute of Biophysics, Consiglio Nazionale delle Ricerche, 20133 Milan, Italy (A.C.)

In planta, very limited information is available about how the endoplasmic reticulum (ER) contributes to cellular Ca^{2+} dynamics and homeostasis. Here, we report the generation of an ER-targeted Cameleon reporter protein suitable for analysis of Ca^{2+} accumulation and dynamics in the lumen of the ER in plant cells. Using stably transformed Arabidopsis (*Arabidopsis thaliana*) plants expressing this reporter protein, we observed a transiently enhanced accumulation of Ca^{2+} in the ER in response to stimuli inducing cytosolic Ca^{2+} rises in root tip cells. In all experimental conditions, ER Ca^{2+} dynamics were substantially different from those monitored in the cytosol. A pharmacological approach enabled us to evaluate the contribution of the different ER-resident Ca^{2+}-ATPase classes in the regulation of the ER Ca^{2+} homeostasis. Taken together, our results do not provide evidence for a role of the ER as a major source that releases Ca^{2+} for stimulus-induced increases in cytosolic Ca^{2+} concentration. Instead, our results show that the luminal ER Ca^{2+} elevations typically follow cytosolic ones, but with distinct dynamics. These findings suggest fundamental differences for the function of the ER in cellular Ca^{2+} homeostasis in plants and animals.

In plants, rises in cytosolic Ca^{2+} concentration ($[Ca^{2+}]_{cyt}$) occur in response to both biotic and abiotic stimuli (Hetherington and Brownlee, 2004; McAinsh and Pittman, 2009; Kudla et al.., 2010; Bose et al., 2011). Depending on the stimulus, these rises can display the form of a single transient or repetitive Ca^{2+} oscillations and are commonly designated as "Ca^{2+} signatures" (Webb et al., 1996; Allen et al., 2000, 2001; Sanders et al., 2002; Young et al., 2006; Kudla et al., 2010).

The generation and shaping of $[Ca^{2+}]_{cyt}$ signatures depends on fine-tuning of Ca^{2+} influxes and effluxes occurring at both the plasma membrane (PM) and membranes of the different subcellular compartments (Pittman and Hirschi, 2003; Hetherington and Brownlee, 2004; Dodd et al., 2010; Spalding and Harper, 2011). The opening of Ca^{2+}-permeable influx channels in response to a stimulus will release Ca^{2+} into the cytosol and cause the generation of a Ca^{2+} spike, while the activity of Ca^{2+} efflux transporters (H^+-Ca^{2+} antiporters and Ca^{2+}-ATPases) will return the $[Ca^{2+}]_{cyt}$ to resting concentrations (McAinsh and Pittman, 2009; Bonza and De Michelis, 2011; Spalding and Harper, 2011).

Recently, the development and application of genetically encoded Ca^{2+} reporter proteins like Cameleons has allowed the study of Ca^{2+} dynamics in several compartments with organ, tissue, and single-cell resolution (Allen et al., 1999; Monshausen et al., 2008; Yang et al., 2008; Sieberer et al., 2009; Costa et al., 2010; Rincón-Zachary et al., 2010; Tanaka et al., 2010; Michard et al., 2011; Krebs et al., 2012; Loro et al., 2012; Behera et al., 2013). Cameleons are fluorescence resonance energy transfer (FRET)-based indicators in which two GFP variants, cyan fluorescent protein (CFP) and yellow fluorescent protein (YFP; or circularly permuted variants of YFP), are linked together by the Ca^{2+}-binding protein calmodulin (CaM) and a CaM-binding peptide (Miyawaki et al., 1997). Binding of Ca^{2+} to the Ca^{2+}-responsive elements alters the efficiency of FRET, allowing for quantitative measurements of Ca^{2+} dynamics. Different Cameleon variants have been developed since the first report about this reporter protein (Miyawaki et al., 1997). This involved, for example, advanced versions with improved fluorescence, larger changes in FRET upon Ca^{2+} binding, and a broad range of Ca^{2+} affinities (Palmer and Tsien, 2006). Moreover, mutational modification of the original Cameleon in the case of the

[1] This work was supported by Ministero dell'Istruzione, dell'Università e della Ricerca Fondo per gli Investimenti della Ricerca di Base (grant no. 2010 RBFR10S1LJ_001 to A.C.), by the German Research Foundation (grant nos. FOR 964 and SFB 629 to J.K.), by the International Max Planck Research School-Cell Dynamics and Disease (Ph.D. fellowship to S.B.), and by a binational Deutscher Akademischer Austausch Dienst/VIGONI grant.

[2] These authors contributed equally to the article.

* Address correspondence to alex.costa@unimi.it.

The author responsible for distribution of materials integral to the findings presented in this article in accordance with the policy described in the Instructions for Authors (www.plantphysiol.org) is: Alex Costa (alex.costa@unimi.it).

[C] Some figures in this article are displayed in color online but in black and white in the print edition.

[W] The online version of this article contains Web-only data.

www.plantphysiol.org/cgi/doi/10.1104/pp.113.226050

D family of indicators ensured that their function is no longer perturbed by large excesses of native CaM (Palmer et al., 2006). The use of Cameleons in plants has allowed the study of cytosolic (Krebs et al., 2012), nuclear (Sieberer et al., 2009; Krebs et al., 2012), peroxisomal (Costa et al., 2010, 2013), and mitochondrial (Loro et al., 2012, 2013) Ca^{2+} dynamics in specific plant organs and single cells. However, despite all these advances, very limited data have been reported regarding in vivo analyses of endoplasmic reticulum (ER) Ca^{2+} dynamics in plants (Iwano et al., 2009).

In animal cells, the ER represents an important Ca^{2+} storage organelle in which the free Ca^{2+} concentration varies between 50 and 500 μM (Coe and Michalak, 2009). Ca^{2+} release from the ER is involved in many different processes, including exocytosis, contraction, metabolism, regulation of transcription, fertilization, and apoptosis. The major Ca^{2+} entry pathway in electrically nonexcitable cells is represented by the "store-operated Ca^{2+} entry" (SOCE; Feske et al., 2012). Here, PM-localized calcium release-activated channels are activated in response to the emptying of intracellular ER Ca^{2+} stores (Parekh and Putney, 2005; Carrasco and Meyer, 2010). Moreover, in several mammalian cell types upon stimulation, Ca^{2+} is released from the ER into the cytosol through the activity of different classes of ER-resident Ca^{2+}-permeable channels activated by second messengers such as inositol 1,4,5-trisphosphate (IP3) and cyclic adenosine diphosphoribose (Parekh and Putney, 2005; Berridge, 2009; Galione and Chuang, 2012). In sharp contrast, for plant cells, no precise data on ER Ca^{2+} concentration ($[Ca^{2+}]_{ER}$) are available (Stael et al., 2012), and in vivo investigations about the Ca^{2+} storage properties of the ER have remained very limited (Iwano et al., 2009).

Moreover, SOCE has not been reported in plants, and stromal interaction molecule (STIM) proteins, which are central components of SOCE, are not encoded in the genomes of higher plants (Collins and Meyer, 2011). Despite some biochemical evidence for Ca^{2+} release in response to IP3, nicotinic acid adenine dinucleotide phosphate, and cyclic adenosine diphosphoribose (Muir and Sanders, 1997; Navazio et al., 2000, 2001), electrophysiological analyses supporting the existence of voltage-gated ER-localized Ca^{2+} channels (Klüsener et al., 1995, 1997), homologous for the respective IP3 and ryanodine receptors, are missing in higher plants (Wheeler and Brownlee, 2008; Kudla et al., 2010). All considered, this situation suggests that the role of the ER for cellular Ca^{2+} dynamics may be fundamentally different in plants as compared with animal cells.

Plants contain two major types of Ca^{2+} pumps named ECA (for ER-type Ca^{2+}-ATPase) and ACA (for autoinhibited Ca^{2+}-ATPase; Geisler et al., 2000; Sze et al., 2000; Bonza and De Michelis, 2011). Plant genomes encode different isoforms of both ECAs and ACAs. These are often coexpressed in certain cell types, and consequently, different cellular membranes in the same cell contain multiple Ca^{2+}-ATPase isoforms (Bonza and De Michelis, 2011). In Arabidopsis (*Arabidopsis thaliana*), immunological and membrane fractionation studies provided evidence for an ER localization of at least two distinct Ca^{2+} pumps, ECA1 and ACA2 (Liang et al., 1997; Harper et al., 1998; Liang and Sze, 1998; Hong et al., 1999; Hwang et al., 2000). Moreover, additional ECA and ACA isoforms are predicted to be ER localized (Geisler et al., 2000; Sze et al., 2000, Baxter et al., 2003; Bonza and De Michelis, 2011). Biochemical characterization revealed that ECA1 and ACA2, besides different regulatory properties, also have different affinities for Ca^{2+}, with one-half saturation concentration for free Ca^{2+} in the submicromolar and micromolar range, respectively (Liang and Sze, 1998; Hwang et al., 2000; Sze et al., 2000; Wu et al., 2002; Bonza and De Michelis, 2011), suggesting their participation in different aspects of ER Ca^{2+} regulation. The main predicted function for the ER Ca^{2+}-ATPases is Ca^{2+} loading into the ER lumen (Corbett and Michalak, 2000; Persson and Harper, 2006). However, how exactly these ER Ca^{2+}-ATPases contribute to ER and cytosolic Ca^{2+} dynamics awaits further investigation.

Here, we report the successful development and application of a genetically encoded Cameleon Ca^{2+} reporter protein for the in vivo analyses of Ca^{2+} dynamics in the ER lumen of Arabidopsis by the combination of mammalian and plant targeting signals. Using this tool, we were able to monitor ER Ca^{2+} dynamics in root cells with organ, tissue, and cell resolution. This approach allowed us to evaluate in vivo the contribution of the different Ca^{2+}-ATPase classes in $[Ca^{2+}]_{ER}$ homeostasis. Taken together, our data do not support a role of the ER as a major Ca^{2+}-releasing source for stimulus-induced increases in cytosolic Ca^{2+} concentration. Instead, our results show that the luminal ER Ca^{2+} transients typically follow cytosolic increases, but with distinct dynamics. These findings suggest fundamental differences for the function of the ER in cellular Ca^{2+} homeostasis in plants and animals.

RESULTS AND DISCUSSION

Generation of a Cameleon-Based Reporter Protein for Monitoring Ca^{2+} Dynamics in the ER of Plants

In order to enable analyses of Ca^{2+} dynamics in the ER of plant cells, we first took advantage of the available D1ER Cameleon Ca^{2+} reporter protein that had already been successfully used to study Ca^{2+} dynamics in the ER of mammalian cells (Palmer et al., 2004; Luciani et al., 2009; Jiménez-Moreno et al., 2010). In this reporter construct, fusion of the D1 reporter protein with a mammalian calreticulin signal sequence and a KDEL ER-retention signal results in specific localization of the Ca^{2+} reporter protein to the mammalian ER (Palmer et al., 2004). Although a modified version of D1ER (CRT-D1ER) was correctly localized at the ER in plant cells, we could detect neither an increase nor a decrease of $[Ca^{2+}]_{ER}$ in response to specific stimuli (for details concerning construct production and localization analysis, see Supplemental Text S1 and Supplemental Fig. S1, respectively).

Since D1 Cameleon has a biphasic Ca^{2+} dependency in vitro (dissociation constant = 0.8 and 60 μM; Palmer and Tsien, 2006), we supposed that the resting $[Ca^{2+}]_{ER}$ in the analyzed cells was above these values. Therefore, we decided to evaluate an alternative probe with a different affinity for Ca^{2+}. The Cameleon D4 variant has an in vitro dissociation constant for Ca^{2+} of 195 μM (Palmer et al., 2006) and was very recently used by two groups to monitor free Ca^{2+} levels in the ER lumen of mammalian cells (Ravier et al., 2011; Kipanyula et al., 2012). To efficiently target the D4 probe to the lumen of plant cell ER, we followed the same cloning strategy adopted for the production of the CRT-D1ER construct. The Arabidopsis CALRETICULIN1A (Christensen et al., 2010) signal peptide was fused upstream of the D4ER Cameleon reporter (Kipanyula et al., 2012), and the entire coding sequence was placed under the control of a single cauliflower mosaic virus (CaMV) 35S promoter. The resulting construct, CRT-D4ER (Fig. 1), was transiently expressed in tobacco (*Nicotiana benthamiana*) leaf epidermal cells (Fig. 1, A–C). Comparison with the localization of nWAK2-mCherry-HDEL (for a full description of the construct, see Nelson et al., 2007) as an ER marker that was coexpressed in these cells revealed that nWAK2-mCherry-HDEL and CRT-D4ER fluorescences fully merged in the nuclear envelope of tobacco epidermal cells (Fig. 1, C and D). The CRT-D4ER reporter construct was subsequently transformed into Arabidopsis plants, and 15 independent stable transgenic lines were selected. Figure 1, E to H, provides representative images of CRT-D4ER Arabidopsis transgenic plants, demonstrating that the probe was expressed in root (Fig. 1E), hypocotyl (Fig. 1F), and mature leaf cells (Fig. 1G). In these different tissues/organs, the typical ER morphology was clearly recognized (Boevink et al., 1999; Brandizzi et al., 2002), with 1- to 5-μm ER fusiform bodies (Hawes et al., 2001; Matsushima et al., 2002, 2003; Nelson et al., 2007) detected in the hypocotyl cells (Fig. 1G). The CRT-D4ER probe was also abundantly expressed in guard cells (Fig. 1, G and H). In order to investigate the Ca^{2+} reporter protein conformation status in resting conditions, we imaged the root tip of transgenic CRT-D4ER seedlings by means of a wide-field fluorescence microscope (excited with a 436/20-nm light wavelength) for the simultaneous acquisition of the CFP and YFP emission wavelengths. In root tip cells expressing CRT-D4ER, the fluorescences of both CFP and the FRET acceptor (YFP in the D4) were detected and were clearly above the level of organ autofluorescence (Fig. 1, I and J). Similar results were obtained by confocal microscopic analysis performed both in leaves and root cells (data not shown).

CRT-D4ER Allows the Visualization of ER Ca^{2+} Dynamics in Root Cells

Subsequently, we sought to use CRT-D4ER to visualize potential variations in $[Ca^{2+}]_{ER}$ in response to defined stimuli. To this end, we challenged 7-d-old Arabidopsis seedlings with different stimuli reported to induce cytosolic Ca^{2+} rises in root cells, such as external ATP (Tanaka et al., 2010; Loro et al., 2012, 2013), L-Glu (Qi et al., 2006), and NaCl (Kiegle et al., 2000). To allow for comparison with cytosolic Ca^{2+} dynamics and as a control for the efficiency of stimulus applications, we performed a series of parallel experiments using either seedlings expressing the cytosol-localized Cameleon YC3.6 (NES-YC3.6; Nagai et al., 2004; Krebs et al., 2012) or expressing CRT-D4ER (Fig. 2).

One millimolar L-Glu was able to stimulate a fast and transient $[Ca^{2+}]_{cyt}$ increase in root tip cells (Fig. 2, A and G). In particular, L-Glu triggered a response in the cells of the root tip region, and then Ca^{2+} elevations spread out quickly to the upper root tip cells (Fig. 2A; Supplemental Movies S1 and S2). The L-Glu-Ca^{2+}-induced elevation is probably dependent on the activity of members of the ionotropic Glu receptors, channels that have been demonstrated to facilitate Ca^{2+} influx across the PM (Michard et al., 2011; Vincill et al., 2012, 2013). Several members of this large family (20 members in Arabidopsis; Lacombe et al., 2001) are in fact expressed in the different tissues of root tip, as reported by published microarray and experimental data (Winter et al., 2007; Vincill et al., 2013).

The same stimulus also triggered a concomitant increase of $[Ca^{2+}]_{ER}$ (Fig. 2, B and G), which was more sustained compared with the rise observed in the cytosol (Fig. 2, B and H). Importantly, separate analyses of the two CFP and FRET fluorescences revealed an evident FRET response, manifested by a decrease of CFP and an increase of YFP emissions (Supplemental Fig. S2A).

A similar series of experiments was then performed with the addition of 0.5 mM ATP (Fig. 2, C and D). In agreement with previous reports, high extracellular ATP concentration resulted in a strong and sustained $[Ca^{2+}]_{cyt}$ increase, with a typical dynamics consisting of different sequential Ca^{2+} peaks due to the influx of external Ca^{2+} and the release of Ca^{2+} from nonidentified internal stores (Fig. 2C; Supplemental Movie S3; Tanaka et al., 2010; Loro et al., 2012). This stimulus also induced an ER Ca^{2+} accumulation (Fig. 2D) in which the maximum level of $[Ca^{2+}]_{ER}$ was reached later as compared with the cytosol (Fig. 2G) but was stronger and even more sustained as compared with the one induced by L-Glu (Fig. 2, D, H, and I). In none of these experiments did we observe a measurable reduction in $[Ca^{2+}]_{ER}$ before the occurrence of the $[Ca^{2+}]_{cyt}$ increase. To further address this aspect, a series of experiments was performed with 0.01 mM ATP, a concentration reported to stimulate ER Ca^{2+} release in HeLa cells (Palmer et al., 2004). As reported previously, root tip cells stimulated with 0.01 mM ATP displayed $[Ca^{2+}]_{cyt}$ dynamics, albeit of lower magnitude (Supplemental Fig. S3, A and C–E; Loro et al., 2012). However, again, only an increase in $[Ca^{2+}]_{ER}$ was observed (Supplemental Fig. S3, B–E). These results strongly support the conclusion that the ER does not represent the internal Ca^{2+}-releasing store involved in the generation of the ATP-induced cytosolic

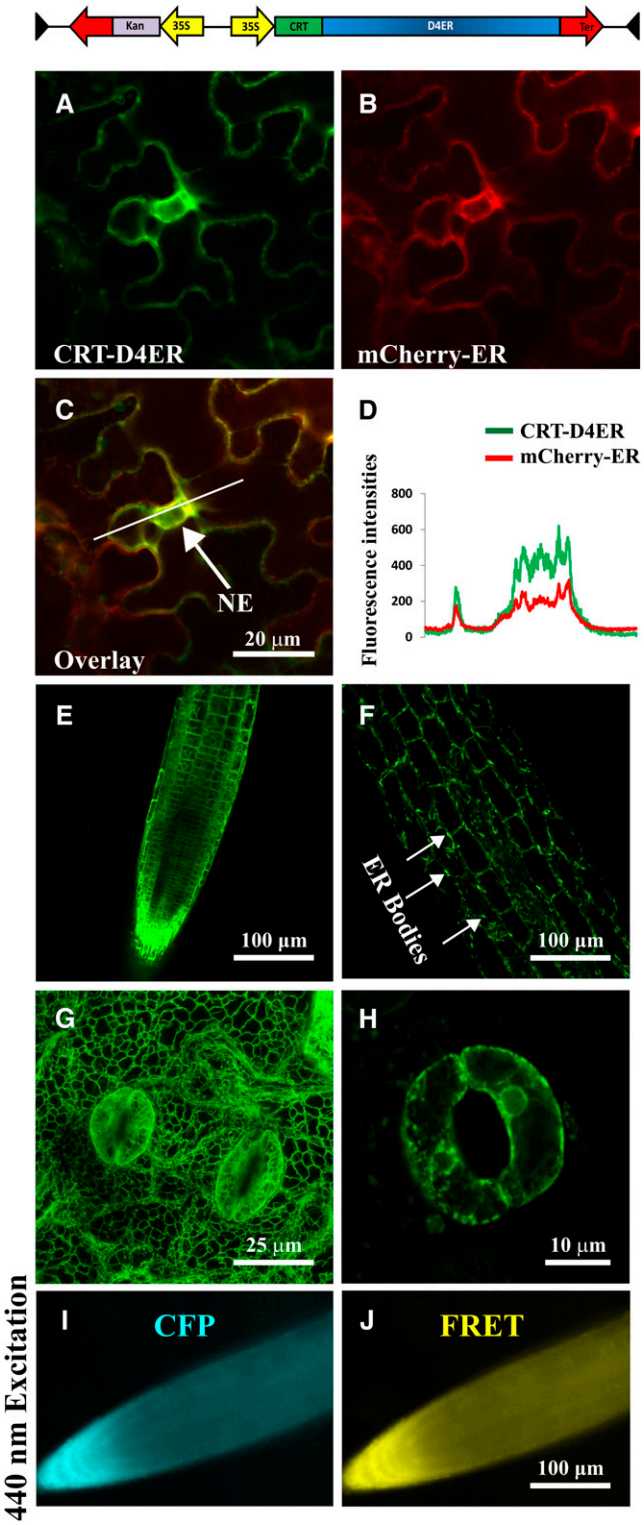

Figure 1. Subcellular distribution of CRT-D4ER in plant cells and simultaneous detection of CFP and FRET emissions. The top panel shows a schematic structure of the CRT-D4ER Cameleon probe. A to C, Confocal images of tobacco agroinfiltrated epidermal cells cotransformed with CRT-D4ER and the ER marker nWAK2-mCherry-HDEL (Nelson et al., 2007). A, Cameleon YFP fluorescence in tobacco epidermal cells. B, mCherry fluorescence in the same cells shown in A. C, The YFP signal of CRT-D4ER colocalizes with mCherry, as revealed by colocalization of the two fluorescence signals at the level of the nuclear envelope (NE). D, Plot profile of YFP and mCherry fluorescences corresponding to the marked white line shown in C. E to H, Confocal microscopy analyses revealed efficient CRT-D4ER YFP expression in different organs of Arabidopsis stable transgenic plants with a subcellular distribution showing typical ER features. E, Root tip cells. F, Hypocotyl cells, showing the presence of fusiform bodies. G, Three-dimensional maximum projection of a mature leaf region. H, Stomata guard cells. I and J, Representative root tip of a CRT-D4ER seedling excited with 440-nm light for FRET detection. I, CFP emission. J, FRET emission. The simultaneous detection of the two emissions demonstrates that CFP was not quenched and YFP was properly excited trough FRET.

Ca^{2+} dynamics. Finally, salt stress was analyzed as a third stimulus that is known to elicit an increase in cytosolic Ca^{2+} in root cells. The effect of NaCl was analyzed in the root mature zone, since these cells respond in a more pronounced manner than root tip cells to salt stress (data not shown). The addition of 100 mM NaCl induced a fast cytosolic Ca^{2+} increase (Fig. 2, E and G), which was accompanied by a Ca^{2+} accumulation in the ER (Fig. 2, F, H, and I). In the latter case, the source of cytosolic Ca^{2+} has been demonstrated to be both from extracellular and intracellular calcium stores, mainly from vacuole (Knight et al., 1997). Our results indeed demonstrate that the ER is not part of such intracellular stores. Moreover, it is worth noting that, compared with the response to L-Glu (Fig. 2, G–I), the increases in $[Ca^{2+}]_{cyt}$ were similar in terms of peak intensities and duration, while the ER Ca^{2+} accumulation induced by NaCl treatment was smaller. This observation could be related to the fact that cells of the root mature zone have extensive vacuoles compared with the meristematic cells of the root tip, hence probably also contributing to Ca^{2+} sequestration (Peiter, 2011).

Altogether, these results indicate that plant cells transiently accumulate Ca^{2+} in the ER in response to different stimuli, similar to what was observed in the apoplast and mitochondria (Gao et al., 2004; Loro et al., 2012). The subsequent decrease in $[Ca^{2+}]_{ER}$, which is especially evident with L-Glu, low ATP concentration, and NaCl treatments, occurs only after the initial accumulation and is likely to be dependent on the activity of ER membrane-resident Ca^{2+}-permeable channels (Klüsener et al., 1995, 1997; Muir and Sanders, 1997; Navazio et al., 2000, 2001). Importantly, these results suggest that, at least in the cases investigated here, the ER does not contribute to the generation of the observed cytosolic Ca^{2+} increases by releasing Ca^{2+}. Instead, it appears that the ER represents a system that mimics $[Ca^{2+}]_{cyt}$ increases, but with distinct dynamics, as marked by the different times at which the peaks of $[Ca^{2+}]_{cyt}$ and $[Ca^{2+}]_{ER}$ are reached after the stimuli perception (Fig. 2G). The delayed ER Ca^{2+} accumulation was particularly evident in ATP-stimulated cells (Fig. 2H; Supplemental Fig. S3E). These dynamics of ER Ca^{2+} accumulation may reflect the intrinsic properties

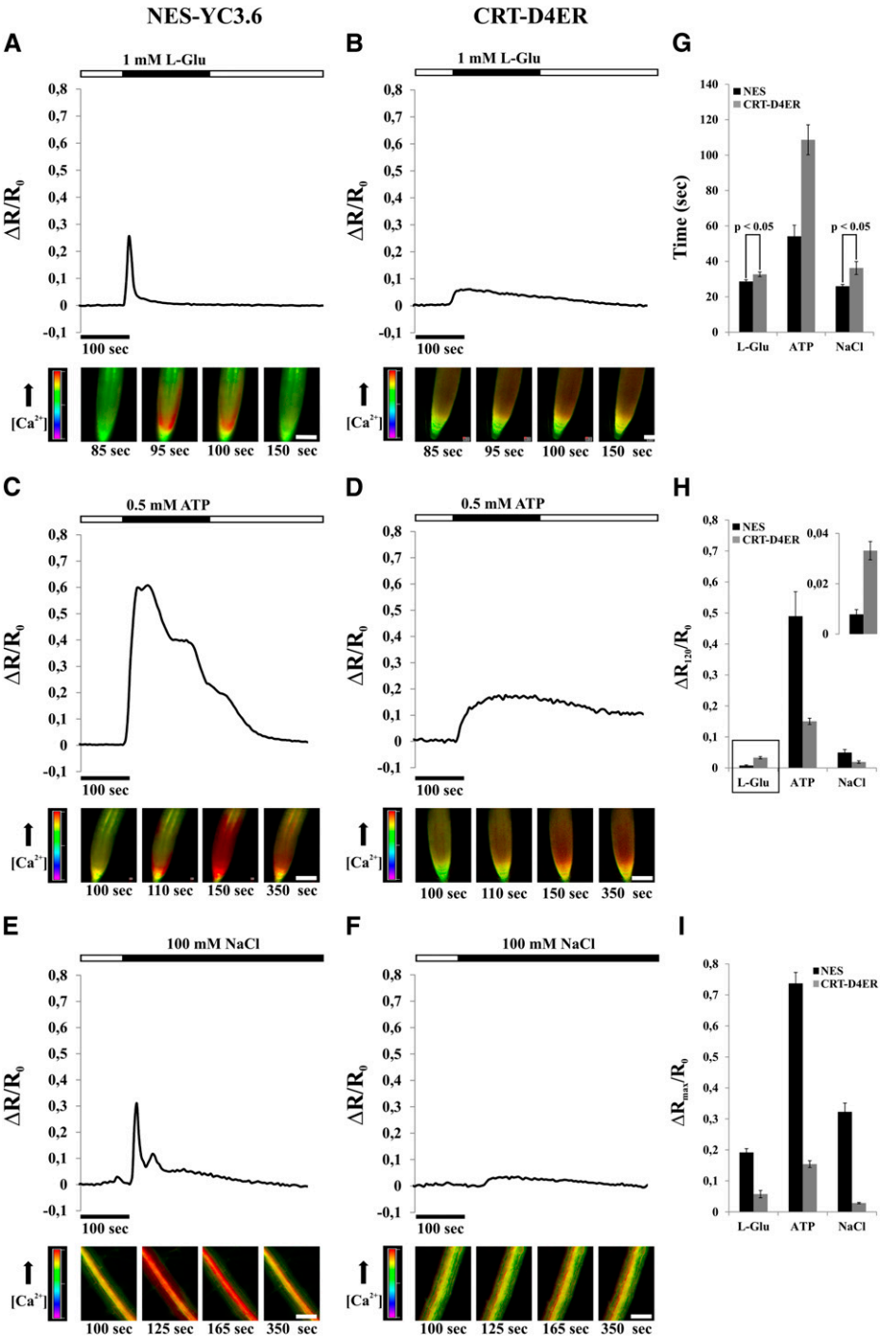

Figure 2. $[Ca^{2+}]_{cyt}$ and $[Ca^{2+}]_{ER}$ monitoring in roots of Arabidopsis seedlings expressing the NES-YC3.6 (cytosolic Cameleon) and CRT-D4ER (ER Cameleon) probes, challenged with different stimuli (L-Glu, ATP, and NaCl) for the indicated times (black rectangles above traces) and analyzed with a wide-field fluorescence microscope. Traces represent the normalized ratio (FRET/CFP) variations observed during the entire experiment. Images at bottom are representative ratio images of the experiment shown in the corresponding trace above. A, L-Glu (1 mM) induced a single steep and fast Ca^{2+} transient in the cytosol of root tip cells. B, The same stimulus of A induced an ER Ca^{2+} accumulation showing a slow kinetic and a sustained Ca^{2+} recovery phase. C, ATP (0.5 mM) induced a strong cytosolic Ca^{2+} transient in the cytosol of root tip cells, where different peaks were recognizable. The recovery phase was more sustained compared with 1 mM L-Glu. D, The same stimulus of C induced an ER Ca^{2+} accumulation showing a slow kinetic, but with values about four times higher than those observed with 1 mM L-Glu and, afterward, with a small $[Ca^{2+}]_{ER}$ decrease. E, NaCl (100 mM) induced a biphasic cytosolic Ca^{2+} response with two peaks of different intensities in cells of the root mature zone. F, The same salt concentration of E led to a small ER Ca^{2+} accumulation followed by a slow $[Ca^{2+}]_{ER}$ decrease. G, Statistical analysis of times at which the maximum $\Delta R/R_0$ variations were measured in both compartments in response to different applied stimuli. H, Statistical analysis of $\Delta R/R_0$ variations measured in both compartments 120 s after sensing of the different applied stimuli. The inset shows a magnification of L-Glu Ca^{2+} peak averages. I, Statistical analysis of maximum $\Delta R/R_0$ variations measured in both compartments in response to different applied stimuli. *P* values were calculated using Student's *t* test. Bars = 100 μm. [See online article for color version of this figure.]

of the ER-resident active Ca^{2+} transport systems (Bonza and De Michelis, 2011; Bose et al., 2011). Instead, the $[Ca^{2+}]_{cyt}$ increase is mainly dependent on the activity of channels occurring at very much faster rate than transporters.

To corroborate that Ca^{2+} accumulation in the ER mimics cytosolic Ca^{2+} rises, we performed a series of experiments in which two different ATP concentrations were applied successively (0.01 mM followed by 0.5 mM) to root tip cells (Fig. 3). In particular, the second administration was applied before both $[Ca^{2+}]_{cyt}$ and $[Ca^{2+}]_{ER}$ were completely recovered to resting values. Figure 3A reports the superimposition of representative normalized ratio variations measured in the cytosol and ER, clearly showing that, in correspondence with each $[Ca^{2+}]_{cyt}$ rise, a $[Ca^{2+}]_{ER}$ rise occurs. Hence, the ER is able to accumulate Ca^{2+} at different levels in response to $[Ca^{2+}]_{cyt}$ increases (Fig. 3B), supporting a role in

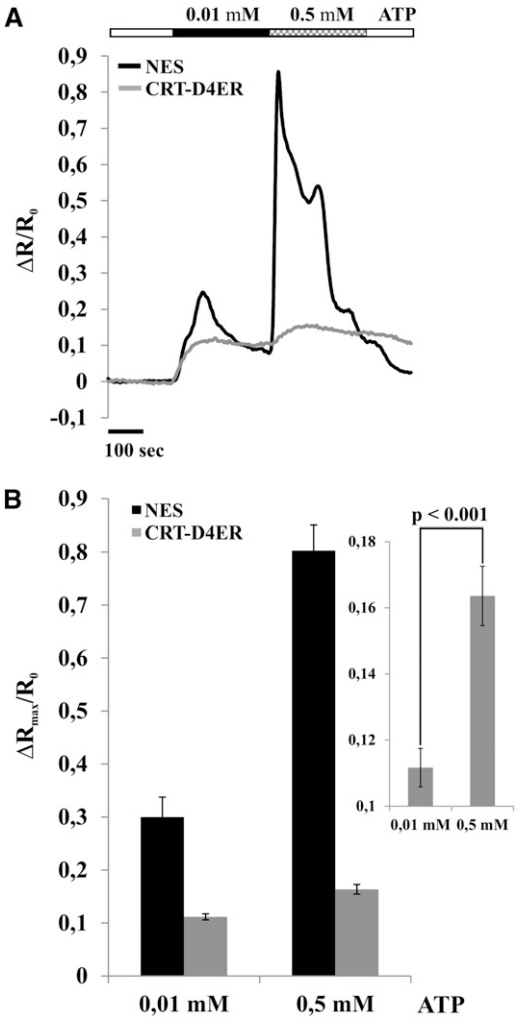

Figure 3. $[Ca^{2+}]_{cyt}$ and $[Ca^{2+}]_{ER}$ monitoring in root tips of Arabidopsis seedlings expressing the NES-YC3.6 (cytosolic Cameleon) and CRT-D4ER (ER Cameleon) probes challenged with 0.01 and 0.5 mM ATP for the indicated times (black and checkered rectangles above traces) and analyzed with a wide-field fluorescence microscope. A, Superimposition of representative normalized ratio variations for each transgenic line. B, Statistical analysis of maximum $\Delta R/R_0$ variations measured in both compartments. The inset shows a magnification of Ca^{2+} peak averages measured in the ER in response to 0.01 and 0.5 mM ATP. *P* values were calculated using Student's *t* test.

buffering the cytosolic Ca^{2+} rises. Together, these results indicate that Ca^{2+} accumulation in the ER is strictly dependent on the $[Ca^{2+}]_{cyt}$.

Finally, when root cells were challenged with a series of hyperpolarizing-depolarizing buffers, known to induce repetitive cytosolic Ca^{2+} transients in guard and root cells (Allen et al., 2000, 2001; Weinl et al., 2008; Krebs et al., 2012), repetitive ER Ca^{2+} accumulations were also observed (Supplemental Fig. S4, A and B). Chelating extracellular Ca^{2+} with EGTA prevented both cytosolic and ER Ca^{2+} transients (Supplemental Fig. S4, C and D), confirming that the ER does not contribute as an intracellular Ca^{2+} store to the generation of stimulus-induced cytosolic Ca^{2+} rises observed. However, we can currently not fully exclude that localized Ca^{2+} releases from ER occur in specific microdomains of cells (Rizzuto and Pozzan, 2006). Based on our microscope resolution, the predominant response of a defined population of root tip cells was measurable that consequently represents the predominant component of ER Ca^{2+} dynamics in these cells.

Comparison of ER Ca^{2+} dynamics induced in root tip cells by L-Glu and ATP revealed that Ca^{2+} accumulation in the ER was directly dependent on the magnitude of cytosolic Ca^{2+} elevation, with ATP inducing the strongest increase (compare the $\Delta R/R_0$ in Fig. 2, B, D, and I). In particular, the observed differences between the responses of root tip cells to L-Glu and ATP may result from a different number of cells responding primarily or secondarily to the stimulus (see the image sequences below the graphs in Fig. 2). In each single cell, the two stimuli may produce an increase in $[Ca^{2+}]_{ER}$ of different amplitude. In order to appreciate Ca^{2+} dynamics in single cells, we performed an analysis of CRT-D4ER-expressing seedlings by means of confocal microscopy. The results, depicted in Figure 4 and Supplemental Movies S4 and S5, demonstrated that amplitudes and dynamics of ER Ca^{2+} transients induced by L-Glu and ATP in single cells essentially reflected the general root tip response. Importantly, these results confirm that our wide-field analyses faithfully reflect the cellular responsiveness of root tip cells to the stimuli investigated.

Altogether, these experiments demonstrate that the CRT-D4ER represents a reliable probe to monitor ER Ca^{2+} dynamics in vivo at both the organ and single-cell levels. Moreover, our results suggest that, in the cells investigated under the conditions examined here, the ER does not represent a major store for releasing Ca^{2+} into the cytosol.

ER-Localized Ca^{2+}-ATPases Modulate ER Ca^{2+} Homeostasis

Having established that dynamic changes in Ca^{2+} accumulation occur in the ER in response to defined stimuli, we next aimed at elucidating the contribution of ER-resident Ca^{2+}-ATPases to $[Ca^{2+}]_{ER}$ homeostasis. In Arabidopsis, members of both classes of Ca^{2+} pumps are resident in the ER membrane (Sze et al., 2000; Bonza and De Michelis, 2011). ECAs are specifically inhibited by cyclopiazonic acid (CPA; Liang and Sze, 1998), while ACAs are particularly sensitive to inhibition by fluorescein derivatives such as erythrosin B or eosin Y (Eos; De Michelis et al., 1993; Geisler et al., 2000; Sze et al., 2000; Bonza et al., 2004; Bonza and De Michelis, 2011). Therefore, in order to evaluate the contribution of the different types of Ca^{2+}-ATPases to ER Ca^{2+} homeostasis, a pharmacological approach was pursued. Published microarray data (Winter et al., 2007) confirmed that root tips of young Arabidopsis seedlings express Ca^{2+} pumps

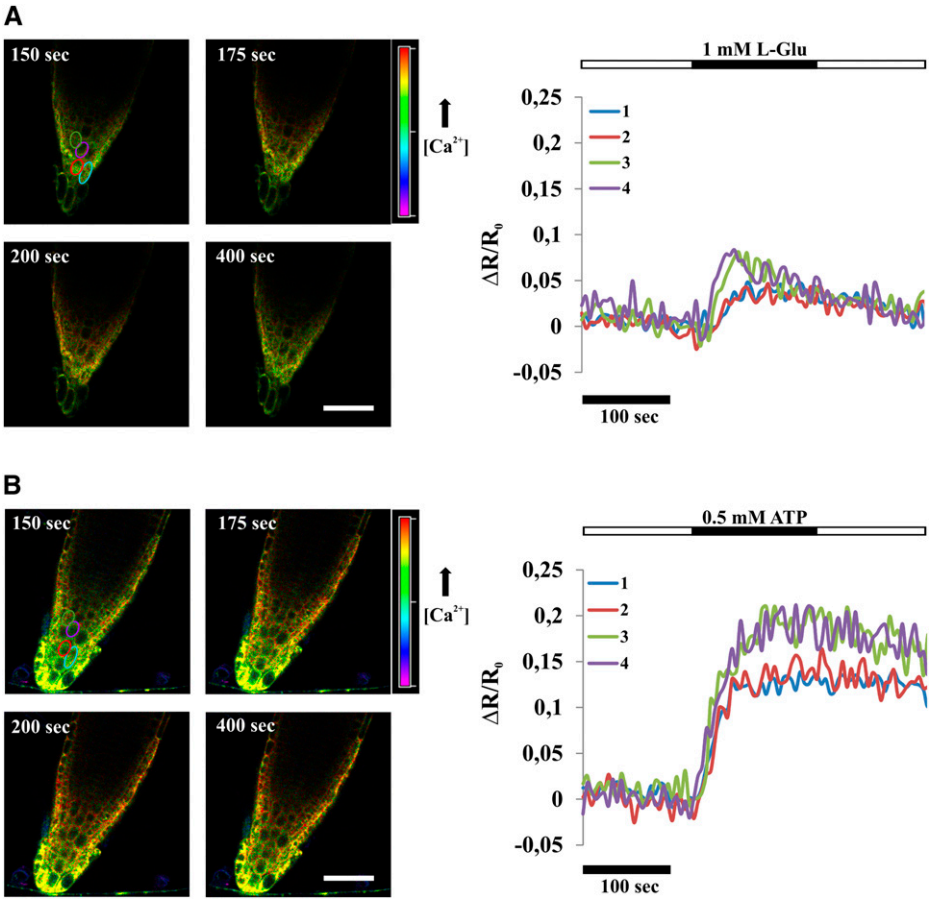

Figure 4. Single-cell $[Ca^{2+}]_{ER}$ monitoring in Arabidopsis CRT-D4ER seedling root tips subjected to L-Glu and ATP for the indicated times (black rectangles above traces). A, Effects of 1 mM L-Glu on the $[Ca^{2+}]_{ER}$ response in Arabidopsis root tip cells. Ratio images for selected frames are shown. B, Effects of 0.5 mM ATP on the $[Ca^{2+}]_{ER}$ response in Arabidopsis root tip cells. Ratio images for selected frames are shown. In both panels, elliptic areas, marked with different colors corresponding to different cells, were used for the ratio calculations (reported as normalized ratio variations $[\Delta R/R_0]$) plotted in the graphs. The two different stimuli triggered responses of different amplitudes, with ATP able to induce higher ER Ca^{2+} accumulations in all analyzed cells compared with L-Glu. Bars = 50 μm.

of both types at various cellular membranes, including the ER-localized Ca^{2+}-ATPase isoforms ACA2 and ECA1 (data not shown).

Arabidopsis seedlings expressing the CRT-D4ER or NES-YC3.6 Cameleon reporter protein were incubated for 10 or 60 min with or without 25 μM CPA, 0.5 μM Eos, and 25 μM CPA plus 0.5 μM Eos. In order to evaluate the $[Ca^{2+}]_{ER}$ and $[Ca^{2+}]_{cyt}$ levels in the different tested conditions, root tips were then analyzed by measuring the ratio values for both CRT-D4ER and NES-YC3.6 probes (Fig. 5). Root tip cells were chosen for the analysis because they harbor smaller vacuoles compared with cells of the mature zone. In this way, we probably reduced the relative contribution of the vacuolar Ca^{2+} transport systems to the regulation of cytosolic Ca^{2+} homeostasis (Cheng et al., 2005; Conn et al., 2011; Peiter, 2011).

The ECA inhibitor CPA affected the CRT-D4ER ratio already after 10 min of treatment, resulting in a significant decrease in the $[Ca^{2+}]_{ER}$ compared with the control condition (Fig. 5A, gray bar). Surprisingly, treatment with the ACA inhibitor Eos did not lead to a $[Ca^{2+}]_{ER}$ decrease but to a $[Ca^{2+}]_{ER}$ increase (Fig. 5A, white bar). Interestingly, when treatments were performed with both inhibitors simultaneously (Fig. 5A, striped bar), the $[Ca^{2+}]_{ER}$ was lower than in the Eos treatment alone but higher than with CPA alone. This suggests that the CPA-sensitive component is just partially responsible for the observed Eos-induced ER Ca^{2+} accumulation. After 60 min of incubation, the results were quite similar with CPA (Fig. 5B, gray bar), while the Eos effect on $[Ca^{2+}]_{ER}$ increases was dramatically enhanced (Fig. 5B, white bar). In the latter condition, the presence of CPA was still able to reduce the $[Ca^{2+}]_{ER}$ (Fig. 5B, striped bar). When the effect of inhibitors was tested on NES-YC3.6 seedlings, we observed that treatment with CPA for 10 min barely affected the $[Ca^{2+}]_{cyt}$ (Fig. 5C, gray bar), while treatment with Eos led to an increase of $[Ca^{2+}]_{cyt}$ (Fig. 5C, gray bar) that was further slightly increased by the simultaneous addition of CPA (Fig. 5C, striped bar). Extension of the treatment to 60 min caused similar, but more pronounced, results.

In summary, the combined analyses of Ca^{2+} dynamics in ER and cytosol with Ca^{2+}-ATPase inhibitors revealed that, under basal conditions, CPA-sensitive ECAs substantially contribute to ER Ca^{2+} accumulation but have a minor role in the control of $[Ca^{2+}]_{cyt}$ levels. Application of Eos compromised the activity of the ACA pumps that are fundamental for the maintenance of basal $[Ca^{2+}]_{cyt}$ in resting conditions but did not prevent the accumulation of Ca^{2+} in the ER, which

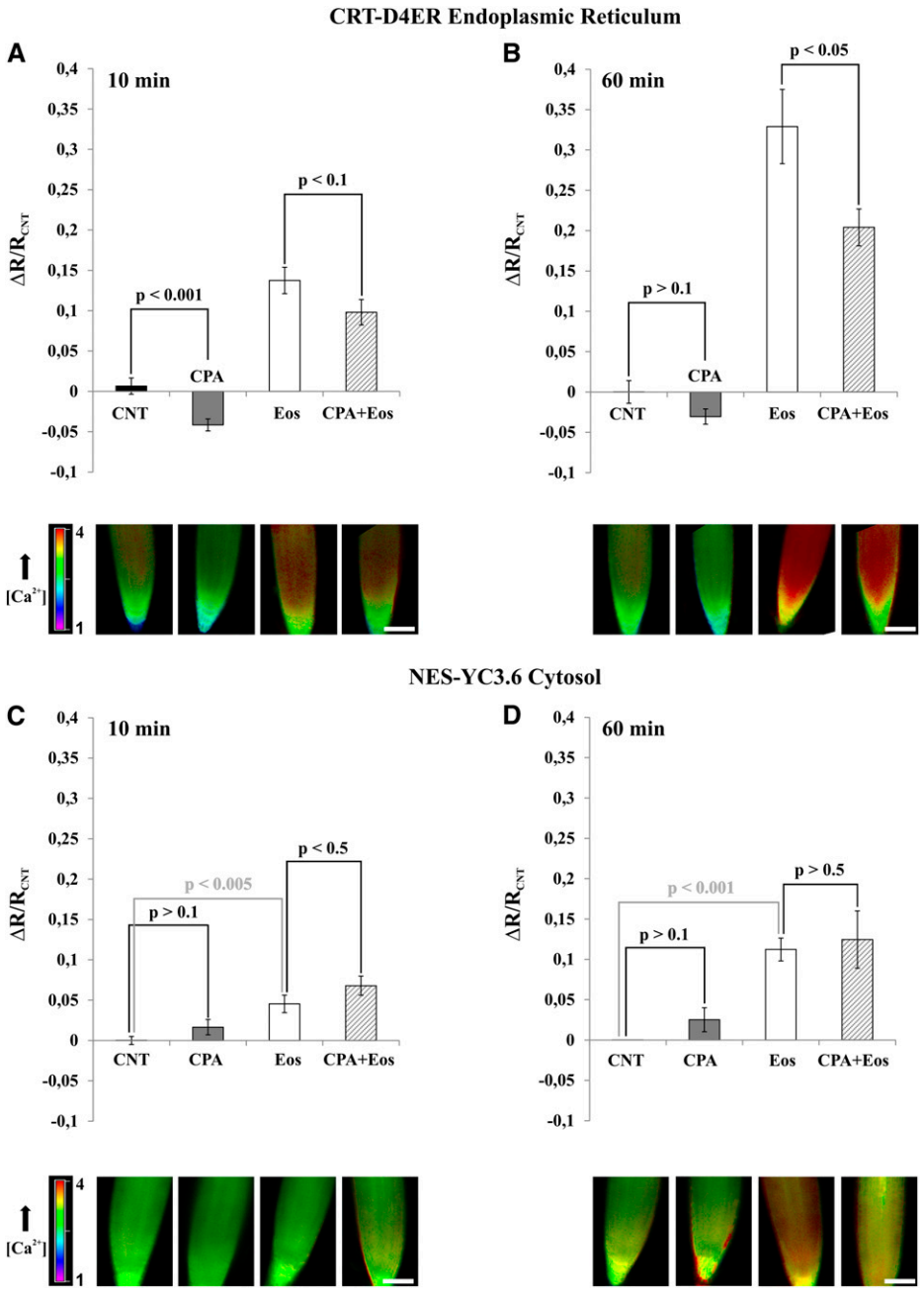

Figure 5. Effects of Ca^{2+}-ATPase inhibitors on $[Ca^{2+}]_{cyt}$ and $[Ca^{2+}]_{ER}$ in root tip cells of Arabidopsis. Seedlings expressing NES-YC3.6 and CRT-D4ER were incubated for 10 and 60 min in control buffer (see "Materials and Methods") or in the presence of 25 μM CPA, 0.5 μM Eos, and 25 μM CPA + 0.5 μM Eos. Root tips were analyzed with a wide-field fluorescence microscope. Bars represent the averaged normalized ratios ($\Delta R/R_{CNT}$) ± SE. The ratios were normalized to the average ratio (R_{CNT}) of each control experiment. The images at bottom are representative ratio images of each tested condition. A and B, $[Ca^{2+}]_{ER}$ Cameleon ratio variations measured in root tip of CRT-D4ER seedlings treated for 10 and 60 min, respectively, with the different inhibitors. C and D, $[Ca^{2+}]_{cyt}$ Cameleon ratio variations measured in root tip of NES-YC3.6 seedlings treated for 10 and 60 min, respectively, with the different inhibitors. *P* values were calculated using Student's *t* test. Bars = 100 μm. [See online article for color version of this figure.]

actually increased. This increase was reduced, but not fully suppressed, by CPA. Considering that under the applied conditions CPA suppressed ECA activity, these results indicate that, under elevated $[Ca^{2+}]_{cyt}$, ECAs contribute to $[Ca^{2+}]_{ER}$ accumulation, but other transport systems are also involved. We cannot exclude that the Eos concentration used in this study was sufficient to inhibit ACA localized at cellular membranes such as PM and tonoplast (Bonza and De Michelis, 2011; Bose et al., 2011) but not fully effective in completely blocking the activity of the ER-resident ACAs (e.g. ACA2; Harper et al., 1998). Hence, it is plausible that the observed elevation of cytosolic Ca^{2+}, due to the inhibition of cytosolic Ca^{2+} removal, leads to higher ER Ca^{2+} accumulation.

CONCLUSION

In this work, we report (1) the generation of the CRT-D4ER Cameleon reporter protein as a suitable tool for the analysis of Ca^{2+} status and dynamics in the ER of plant cells; (2) the analysis of ER Ca^{2+} dynamics in root tip cells in response to defined stimuli; and (3) the evaluation of the contribution of ECA and ACA Ca^{2+}-ATPases to the control of ER Ca^{2+} homeostasis.

The application of CRT-D4ER enables the study of the dynamics of $[Ca^{2+}]_{ER}$ and its interconnection with cytosolic Ca^{2+} signatures in different cell types, genetic backgrounds, and developmental and stress-response processes.

Using this tool, we comparatively analyzed the dynamics of $[Ca^{2+}]_{ER}$ and $[Ca^{2+}]_{cyt}$ in response to different stimuli like ATP, L-Glu, NaCl, and alternate applications of depolarizing and hyperpolarizing buffer. In conclusion, all our data do not support a significant role of $[Ca^{2+}]_{ER}$ as a source of Ca^{2+} release that contributes to the formation of cytosolic Ca^{2+} signatures, at least in the cell types and during the responses investigated in this study. Instead, our data support the hypothesis that, in plant cells, the ER functions primarily as a mimicking system for cytosolic Ca^{2+} signaling. These findings point to fundamental differences in the role of the ER for cellular Ca^{2+} dynamics in plants and animals.

MATERIALS AND METHODS

Plant Material and Growth Conditions

All Arabidopsis (*Arabidopsis thaliana*) plants used in this study were of the Columbia ecotype. Plants were grown on 16/8-h cycles of light (70 μmol m^{-2} s^{-1}) at 22°C and 75% relative humidity. Seeds of Arabidopsis were surface sterilized by vapor-phase sterilization (Clough and Bent, 1998) and plated on one-half Murashige and Skoog medium (Murashige and Skoog medium plus M0222 elements including vitamins; Duchefa [http://www.duchefa-biochemie.nl/]; Murashige and Skoog, 1962) supplemented with 0.1% (w/v) Suc and 0.05% (w/v) MES, pH 6.0, and solidified with 0.8% (w/v) plant agar (Duchefa). After stratification at 4°C in the dark for 3 d, seeds were transferred to the growth chamber with 16/8-h cycles of light (70 μmol m^{-2} s^{-1}) at 24°C. The plates were kept vertically. Seedlings used for the analyses were 7 to 8 d old, which corresponds to an average root length of 3 cm.

DNA Constructs

In order to generate the binary vectors for the expression of the Cameleon ER probes in plants, we inserted the single CaMV 35S promoter and the CaMV poly(A) terminator in the polylinker of the pGreen0029 binary vector (Hellens et al., 2000) by using the *Kpn*I and *Sac*I restriction sites, respectively. The CaMV 35S and CaMV poly(A) were PCR amplified using the 35S-CaMV cassette vector as a template (http://www.pgreen.ac.uk/JIT/JIT_fr.htm) and the following primer pairs: 35S-For, 5′-CATGggtaccGATATCGTACCCCTACTCCA-3′; 35S-Rev, 5′-CATGggtaccGGGCTGTCCTCTCCAAATGAA-3′; Ter-For, 5′-CATGgagctcGGTACGCTGAAATCACCAGT-3′; and Ter-Rev, 5′-CATGgagctcATCGATCTGGATTTTAGTACTGGA-3′ (the sequences of the restriction sites are shown in lower-case letters). D1ER (AY796115.1) and D4ER (Plasmid 37473: pBAD-D4; http://www.addgene.org/37473/) coding sequences were digested from the pcDNA3-D1ER and pcDNA3-D4ER vectors with *Hin*dIII and *Eco*RI restriction enzymes and ligated into the modified pGreen0029-35S-Ter binary vector. In order to generate the CRT-D1ER and CRT-D4ER constructs, the first 66 nucleotides (CRT) of the Arabidopsis CALRETICULIN1A gene (At1g56340) were PCR amplified and fused upstream the D1ER and D4ER coding sequences by using the *Hin*dIII restriction site. The primers used were as follows: CRT-For, 5′-CATGaagcttATGGCGAAACTAAACCCTAAATT-3′; and CRT-Rev, 5′-CATGaagcttgAGCAGAGACGATCACCACGA-3′. The amplicon was isolated by digestion and ligated into the 35S-D1ER and 35S-D4ER linearized vectors. The obtained clones were sequenced to verify the right orientation of the CRT sequence.

The binary vectors were then introduced into the *Agrobacterium tumefaciens* GV3101 strain.

Transgenic Plants and Tobacco Transient Transformation

The *A. tumefaciens* strains obtained as reported above were used to generate transgenic Arabidopsis plants by the floral dip method (Clough and Bent, 1998). For each construct, 15 Arabidopsis independent transgenic lines were selected, and four independent lines were employed for imaging experiments. Experiments were carried out in seedlings of the T1 and T2 generations for CRT-D4ER transgenic lines. Mature T2 plants were affected by silencing. To minimize this problem, work is in progress to test different vector backbones and promoters.

Transient expression of CRT-D4ER in tobacco (*Nicotiana benthamiana*) epidermal leaf cells was performed as described by Waadt and Kudla (2008).

Seedling Preparation for Ca^{2+} Imaging

For root cell imaging, 7-d-old seedlings grown vertically were prepared accordingly to Behera and Kudla (2013) in dedicated chambers and overlaid with wet cotton in order to continuously perfuse the root with the imaging solution (5 mM KCl, 10 mM MES, 10 mM Ca^{2+}, pH 5.8, adjusted with Tris for ATP and L-Glu, or 0.1 mM KCl, 10 mM MES, 1 mM Ca^{2+}, pH 5.8, adjusted with Tris for NaCl). The shoot was not submerged in the solution. L-Glu and ATP were added as disodium or magnesium salt, respectively, to the chamber by perfusion with the same solution. For chemical treatments, seedlings were preincubated for 10 or 60 min in 5-cm petri dishes in the imaging solution supplemented with 25 μM CPA, 0.5 μM Eos, or a combination of both. Control seedlings were kept for the same times in the imaging solution supplemented with 0.25% (v/v) dimethyl sulfoxide. Seedlings were then transferred to the imaging chamber and allowed to recover for approximately 7 min prior to measurement.

Time-Lapse Ca^{2+} Imaging and Confocal Microscopy Analyses

Cameleon seedling roots and leaves were imaged in vivo by an inverted fluorescence Nikon microscope (Ti-E; http://www.nikon.com/) with a CFI planfluor 4× numerical aperture 0.13 dry objective and a CFI PLAN APO 20× VC dry objective. Excitation light was produced by a fluorescent lamp (Prior Lumen 200 PRO; Prior Scientific; http://www.prior.com) at 440 nm (436/20 nm) set to 20%. Images were collected with a Hamamatsu Dual CCD camera (ORCA-D2; http://www.hamamatsu.com/). For Cameleon analysis, the FRET CFP/YFP optical block A11400-03 (emission 1, 483/32 nm for CFP; emission 2, 542/27 nm for FRET) with a dichroic 510-nm mirror (Hamamatsu) was used for the simultaneous CFP and FRET acquisitions (citrine for D1, YFP for D4, and cpVenus for YC3.6). Exposure time was from 100 to 400 ms with a 2 × 2 CCD binning for cytosolic Cameleon (NES-YC3.6) and a 4 × 4 CCD binning for ER Cameleons (CRT-D1ER and CRT-D4ER). Images where acquired every 5 s. Filters and the dichroic mirror were purchased from Chroma Technology (http://www.chroma.com/). NIS-Elements (Nikon; http://www.nis-elements.com/) was used as a platform to control microscope, illuminator, camera, and post-acquisition analyses.

With regard to time-course experiments, fluorescence intensity was determined over regions of interest that correspond to the root tip zone. FRET and CFP emissions of the analyzed regions of interest were used for the ratio (R) calculation (FRET/CFP) and normalized to the initial ratio (R_0) and plotted versus time ($\Delta R/R_0$). The background was independently subtracted for both channels before calculating the ratio.

Confocal microscopy analyses were performed using Nikon C2 (http://www.nikoninstruments.com) and Leica SP5 (http://www.leica-microsystems.com) laser scanning confocal imaging systems. For Cameleon-dependent citrine (D1), YFP (D4), and cpVenus (YC3.6), excitation was at 488 nm and emission was between 525 and 540 nm. For mCherry detection, excitation was at 561 nm and emission was between 590 and 620 nm. Image analyses were done with the ImageJ bundle software (http://rsb.info.nih.gov/ij/).

For Ca^{2+} imaging analyses, roots were imaged with a 63× lens (H 63X PL APO numerical aperture 1.20 water immersion), and the Cameleons were excited with the 458-nm line of the argon laser with 15% of total power. The CFP and FRET emissions were collected at 473 to 505 nm and 526 to 536 nm, respectively, and the pinhole diameter was 2 to 4 airy units depending on the line used. Images were collected every 5 s. The false color ratio images were obtained by using the NIS-Elements (Nikon; http://www.nis-elements.com/). For time-course experiments, fluorescence intensity was determined over regions of interest that correspond to single cells in the root tip zone. FRET and CFP emissions of the analyzed regions of interest were used for the ratio (R) calculation (FRET/CFP) and normalized to the initial ratio (R_0) and plotted versus time ($\Delta R/R_0$).

All the data are representative of at least six independent cells or roots analyzed unless otherwise stated. Reported traces are representative ones

chosen from a set of six or more identical experiments, and the data shown as bar diagrams are averages from corresponding data sets. Data are reported as averages ± SE, and statistical significance was calculated by Student's *t* test.

In Vivo Dynamic Range of CRT-D4ER

In order to determine the in vivo dynamic range of the CRT-D4ER probe ($\Delta R_{max}/R_0$), we considered the R_{min} and R_{max} measured in the experiments performed in root tip seedlings incubated with Ca^{2+}-ATPase inhibitors. The measured R_{min} was 2.71 ± 0.021 in the presence of 25 μM CPA after 10 min of incubation, whereas the R_{max} was 3.78 ± 0.18 in the presence of 0.5 μM Eos for 60 min. Hence, the calculated $\Delta R_{max}/R = 0.395$ shows that the responses to the different observed stimuli did not lead to a probe saturation.

Supplemental Data

The following materials are available in the online version of this article.

Supplemental Figure S1. Subcellular distribution of CRT-D1ER in transgenic Arabidopsis plants and simultaneous detection of CFP and FRET emissions.

Supplemental Figure S2. FRET detection in Arabidopsis seedlings expressing the CRT-D4ER (ER Cameleon) probe challenged with 1 mM L-Glu, 0.1 mM ATP, and 100 mM NaCl.

Supplemental Figure S3. $[Ca^{2+}]_{cyt}$ and $[Ca^{2+}]_{ER}$ dynamics in root cells of Arabidopsis seedlings expressing the NES-YC3.6 (cytosolic Cameleon) and CRT-D4ER (ER Cameleon) probes challenged with 0.01 mM ATP.

Supplemental Figure S4. $[Ca^{2+}]_{cyt}$ and $[Ca^{2+}]_{ER}$ dynamics in root cells of Arabidopsis seedlings expressing the NES-YC3.6 (cytosolic Cameleon) and CRT-D4ER (ER Cameleon) probes challenged with repetitive depolarizing-hyperpolarizing buffer changes in the presence or absence of EGTA.

Supplemental Text S1. Generation and analysis of Arabidopsis plants expressing the CRT-D1ER Cameleon probe.

Supplemental Movie S1. Series of cytosolic Ca^{2+} ratio images (low magnification, 4×) of an Arabidopsis seedling root tip expressing NES-YC3.6 challenged with 1 mM L-Glu.

Supplemental Movie S2. Series of cytosolic Ca^{2+} ratio images of an Arabidopsis seedling root tip expressing NES-YC3.6 challenged with 1 mM L-Glu analyzed by confocal laser scanning microscopy.

Supplemental Movie S3. Series of cytosolic Ca^{2+} ratio images of an Arabidopsis seedling root tip expressing NES-YC3.6 challenged with 0.5 mM ATP analyzed by confocal laser scanning microscopy.

Supplemental Movie S4. Series of ER Ca^{2+} ratio images of an Arabidopsis seedling root tip expressing CRT-D4ER challenged with 1 mM L-Glu analyzed by confocal laser scanning microscopy.

Supplemental Movie S5. Series of ER Ca^{2+} ratio images of an Arabidopsis seedling root tip expressing CRT-D4ER challenged with 0.5 mM ATP analyzed by confocal laser scanning microscopy.

ACKNOWLEDGMENTS

We thank Maria Ida De Michelis (University of Milan) for critical reading of the manuscript; Prof. Anna Moroni (University of Milan) for helpful discussions; Karin Schumacher (University of Heidelberg) for providing us the UBQ10-NES-YC3.6 Arabidopsis plants; Roger Tsien (University of California, San Diego) for providing us the pCDNA3-D1ER vector; and Tullio Pozzan (University of Padova) for the pCDNA3-D1ER vector.

Received August 1, 2013; accepted September 30, 2013; published September 30, 2013.

LITERATURE CITED

Allen GJ, Kwak JM, Chu SP, Llopis J, Tsien RY, Harper JF, Schroeder JI (1999) Cameleon calcium indicator reports cytoplasmic calcium dynamics in Arabidopsis guard cells. Plant J **19:** 735–747

Allen GJ, Chu SP, Schumacher K, Shimazaki CT, Vafeados D, Kemper A, Hawke SD, Tallman G, Tsien RY, Harper JF, et al (2000) Alteration of stimulus-specific guard cell calcium oscillations and stomatal closing in Arabidopsis det3 mutant. Science **289:** 2338–2342

Allen GJ, Chu SP, Harrington CL, Schumacher K, Hoffmann T, Tang YY, Grill E, Schroeder JI (2001) A defined range of guard cell calcium oscillation parameters encodes stomatal movements. Nature **411:** 1053–1057

Baxter I, Tchieu J, Sussman MR, Boutry M, Palmgren MG, Gribskov M, Harper JF, Axelsen KB (2003) Genomic comparison of P-type ATPase ion pumps in Arabidopsis and rice. Plant Physiol **132:** 618–628

Behera S, Krebs M, Loro G, Schumacher K, Costa A, Kudla J (2013) Ca^{2+} imaging in plants using genetically encoded Yellow Cameleon Ca^{2+} indicators. Cold Spring Harb Protoc **2013:** 700–703

Behera S, Kudla J (2013) High-resolution imaging of cytoplasmic Ca^{2+} dynamics in Arabidopsis roots. Cold Spring Harb Protoc **2013:** 665–669

Berridge MJ (2009) Inositol trisphosphate and calcium signalling mechanisms. Biochim Biophys Acta **1793:** 933–940

Boevink P, Martin B, Oparka K, Santa Cruz S, Hawes C (1999) Transport of virally expressed green fluorescent protein through the secretory pathway in tobacco leaves is inhibited by cold shock and brefeldin A. Planta **208:** 392–400

Bonza MC, De Michelis MI (2011) The plant Ca^{2+}-ATPase repertoire: biochemical features and physiological functions. Plant Biol (Stuttg) **13:** 421–430

Bonza MC, Luoni L, De Michelis MI (2004) Functional expression in yeast of an N-deleted form of At-ACA8, a plasma membrane Ca^{2+}-ATPase of *Arabidopsis thaliana*, and characterization of a hyperactive mutant. Planta **218:** 814–823

Bose J, Pottosin II, Shabala SS, Palmgren MG, Shabala S (2011) Calcium efflux systems in stress signaling and adaptation in plants. Front Plant Sci **2:** 85

Brandizzi F, Fricker M, Hawes C (2002) A greener world: the revolution in plant bioimaging. Nat Rev Mol Cell Biol **3:** 520–530

Carrasco S, Meyer T (2010) Cracking CRAC. Nat Cell Biol **12:** 416–418

Cheng NH, Pittman JK, Shigaki T, Lachmansingh J, LeClere S, Lahner B, Salt DE, Hirschi KD (2005) Functional association of Arabidopsis CAX1 and CAX3 is required for normal growth and ion homeostasis. Plant Physiol **138:** 2048–2060

Christensen A, Svensson K, Thelin L, Zhang W, Tintor N, Prins D, Funke N, Michalak M, Schulze-Lefert P, Saijo Y, et al (2010) Higher plant calreticulins have acquired specialized functions in Arabidopsis. PLoS ONE **5:** e11342

Clough SJ, Bent AF (1998) Floral dip: a simplified method for Agrobacterium-mediated transformation of *Arabidopsis thaliana.* Plant J **16:** 735–743

Coe H, Michalak M (2009) Calcium binding chaperones of the endoplasmic reticulum. General Physiology and Biophysics **28:** F96–F103

Collins SR, Meyer T (2011) Evolutionary origins of STIM1 and STIM2 within ancient Ca^{2+} signaling systems. Trends Cell Biol **21:** 202–211

Conn SJ, Gilliham M, Athman A, Schreiber AW, Baumann U, Moller I, Cheng NH, Stancombe MA, Hirschi KD, Webb AA, et al (2011) Cell-specific vacuolar calcium storage mediated by CAX1 regulates apoplastic calcium concentration, gas exchange, and plant productivity in *Arabidopsis*. Plant Cell **23:** 240–257

Corbett EF, Michalak M (2000) Calcium, a signaling molecule in the endoplasmic reticulum? Trends Biochem Sci **25:** 307–311

Costa A, Drago I, Behera S, Zottini M, Pizzo P, Schroeder JI, Pozzan T, Lo Schiavo F (2010) H_2O_2 in plant peroxisomes: an *in vivo* analysis uncovers a Ca^{2+}-dependent scavenging system. Plant J **62:** 760–772

Costa A, Drago I, Zottini M, Pizzo P, Pozzan T (2013) Peroxisome Ca^{2+} homeostasis in animal and plant cells. Subcell Biochem **69:** 111–133

De Michelis MI, Carnelli A, Rasi-Caldogno F (1993) The Ca^{2+} pump of the plasma membrane of *Arabidopsis thaliana*: characteristics and sensitivity to fluorescein derivatives. Bot Acta **106:** 20–25

Dodd AN, Kudla J, Sanders D (2010) The language of calcium signaling. Annu Rev Plant Biol **61:** 593–620

Feske S, Skolnik EY, Prakriya M (2012) Ion channels and transporters in lymphocyte function and immunity. Nat Rev Immunol **12:** 532–547

Geisler M, Axelsen KB, Harper JF, Palmgren MG (2000) Molecular aspects of higher plant P-type Ca^{2+}-ATPases. Biochim Biophys Acta **1465:** 52–78

Galione A, Chuang KT (2012) Pyridine nucleotide metabolites and calcium release from intracellular stores. Adv Exp Med Biol **740:** 305–323

Gao D, Knight MR, Trewavas AJ, Sattelmacher B, Plieth C (2004) Self-reporting Arabidopsis expressing pH and [Ca^{2+}] indicators unveil ion dynamics in the cytoplasm and in the apoplast under abiotic stress. Plant Physiol **134:** 898–908

Harper JF, Hong B, Hwang I, Guo HQ, Stoddard R, Huang JF, Palmgren MG, Sze H (1998) A novel calmodulin-regulated Ca^{2+}-ATPase (ACA2) from Arabidopsis with an N-terminal autoinhibitory domain. J Biol Chem **273:** 1099–1106

Hawes C, Saint-Jore C, Martin B, Zheng HQ (2001) ER confirmed as the location of mystery organelles in Arabidopsis plants expressing GFP! Trends Plant Sci **6:** 245–246

Hellens RP, Edwards EA, Leyland NR, Bean S, Mullineaux PM (2000) pGreen: a versatile and flexible binary Ti vector for Agrobacterium-mediated plant transformation. Plant Mol Biol **42:** 819–832

Hetherington AM, Brownlee C (2004) The generation of Ca^{2+} signals in plants. Annu Rev Plant Biol **55:** 401–427

Hong B, Ichida A, Wang Y, Gens JS, Pickard BG, Harper JF (1999) Identification of a calmodulin-regulated Ca^{2+}-ATPase in the endoplasmic reticulum. Plant Physiol **119:** 1165–1176

Hwang I, Sze H, Harper JF (2000) A calcium-dependent protein kinase can inhibit a calmodulin-stimulated Ca^{2+} pump (ACA2) located in the endoplasmic reticulum of Arabidopsis. Proc Natl Acad Sci USA **97:** 6224–6229

Iwano M, Entani T, Shiba H, Kakita M, Nagai T, Mizuno H, Miyawaki A, Shoji T, Kubo K, Isogai A, et al (2009) Fine-tuning of the cytoplasmic Ca^{2+} concentration is essential for pollen tube growth. Plant Physiol **150:** 1322–1334

Jiménez-Moreno R, Wang ZM, Messi ML, Delbono O (2010) Sarcoplasmic reticulum Ca^{2+} depletion in adult skeletal muscle fibres measured with the biosensor D1ER. Pflugers Arch **459:** 725–735

Kiegle E, Moore CA, Haseloff J, Tester MA, Knight MR (2000) Cell-type-specific calcium responses to drought, salt and cold in the Arabidopsis root. Plant J **23:** 267–278

Kipanyula MJ, Contreras L, Zampese E, Lazzari C, Wong AK, Pizzo P, Fasolato C, Pozzan T (2012) Ca^{2+} dysregulation in neurons from transgenic mice expressing mutant presenilin 2. Aging Cell **11:** 885–893

Klüsener B, Boheim G, Liss H, Engelberth J, Weiler EW (1995) Gadolinium-sensitive, voltage-dependent calcium release channels in the endoplasmic reticulum of a higher plant mechanoreceptor organ. EMBO J **14:** 2708–2714

Klüsener B, Boheim G, Weiler EW (1997) Modulation of the ER Ca^{2+} channel BCC1 from tendrils of *Bryonia dioica* by divalent cations, protons and H_2O_2. FEBS Lett **407:** 230–234

Knight H, Trewavas AJ, Knight MR (1997) Calcium signalling in *Arabidopsis thaliana* responding to drought and salinity. Plant J **12:** 1067–1078

Krebs M, Held K, Binder A, Hashimoto K, Den Herder G, Parniske M, Kudla J, Schumacher K (2012) FRET-based genetically encoded sensors allow high-resolution live cell imaging of Ca^{2+} dynamics. Plant J **69:** 181–192

Kudla J, Batistic O, Hashimoto K (2010) Calcium signals: the lead currency of plant information processing. Plant Cell **22:** 541–563

Lacombe B, Becker D, Hedrich R, DeSalle R, Hollmann M, Kwak JM, Schroeder JI, Le Novère N, Nam HG, Spalding EP, et al (2001) The identity of plant glutamate receptors. Science **292:** 1486–1487

Liang F, Cunningham KW, Harper JF, Sze H (1997) ECA1 complements yeast mutants defective in Ca^{2+} pumps and encodes an endoplasmic reticulum-type Ca^{2+}-ATPase in *Arabidopsis thaliana.* Proc Natl Acad Sci USA **94:** 8579–8584

Liang F, Sze H (1998) A high-affinity Ca^{2+} pump, ECA1, from the endoplasmic reticulum is inhibited by cyclopiazonic acid but not by thapsigargin. Plant Physiol **118:** 817–825

Loro G, Drago I, Pozzan T, Schiavo FL, Zottini M, Costa A (2012) Targeting of Cameleons to various subcellular compartments reveals a strict cytoplasmic/mitochondrial Ca^{2+} handling relationship in plant cells. Plant J **71:** 1–13

Loro G, Ruberti C, Zottini M, Costa A (2013) The D3cpv Cameleon reports Ca^{2+} dynamics in plant mitochondria with similar kinetics of the YC3.6 Cameleon, but with a lower sensitivity. J Microsc **249:** 8–12

Luciani DS, Gwiazda KS, Yang TL, Kalynyak TB, Bychkivska Y, Frey MH, Jeffrey KD, Sampaio AV, Underhill TM, Johnson JD (2009) Roles of IP3R and RyR Ca^{2+} channels in endoplasmic reticulum stress and beta-cell death. Diabetes **58:** 422–432

Matsushima R, Hayashi Y, Kondo M, Shimada T, Nishimura M, Hara-Nishimura I (2002) An endoplasmic reticulum-derived structure that is induced under stress conditions in Arabidopsis. Plant Physiol **130:** 1807–1814

Matsushima R, Kondo M, Nishimura M, Hara-Nishimura I (2003) A novel ER-derived compartment, the ER body, selectively accumulates a beta-glucosidase with an ER-retention signal in Arabidopsis. Plant J **33:** 493–502

McAinsh MR, Pittman JK (2009) Shaping the calcium signature. New Phytol **181:** 275–294

Michard E, Lima PT, Borges F, Silva AC, Portes MT, Carvalho JE, Gilliham M, Liu LH, Obermeyer G, Feijó JA (2011) Glutamate receptor-like genes form Ca^{2+} channels in pollen tubes and are regulated by pistil D-serine. Science **332:** 434–437

Miyawaki A, Llopis J, Heim R, McCaffery JM, Adams JA, Ikura M, Tsien RY (1997) Fluorescent indicators for Ca^{2+} based on green fluorescent proteins and calmodulin. Nature **388:** 882–887

Monshausen GB, Messerli MA, Gilroy S (2008) Imaging of the Yellow Cameleon 3.6 indicator reveals that elevations in cytosolic Ca^{2+} follow oscillating increases in growth in root hairs of Arabidopsis. Plant Physiol **147:** 1690–1698

Muir SR, Sanders D (1997) Inositol 1,4,5-trisphosphate-sensitive Ca^{2+} release across nonvacuolar membranes in cauliflower. Plant Physiol **114:** 1511–1521

Murashige T, Skoog F (1962) A revised medium for rapid growth and bioassays with tobacco tissue cultures. Physiol Plant **15:** 473–497

Nagai T, Yamada S, Tominaga T, Ichikawa M, Miyawaki A (2004) Expanded dynamic range of fluorescent indicators for Ca^{2+} by circularly permuted yellow fluorescent proteins. Proc Natl Acad Sci USA **101:** 10554–10559

Navazio L, Bewell MA, Siddiqua A, Dickinson GD, Galione A, Sanders D (2000) Calcium release from the endoplasmic reticulum of higher plants elicited by the NADP metabolite nicotinic acid adenine dinucleotide phosphate. Proc Natl Acad Sci USA **97:** 8693–8698

Navazio L, Mariani P, Sanders D (2001) Mobilization of Ca^{2+} by cyclic ADP-ribose from the endoplasmic reticulum of cauliflower florets. Plant Physiol **125:** 2129–2138

Nelson BK, Cai X, Nebenführ A (2007) A multicolored set of *in vivo* organelle markers for co-localization studies in Arabidopsis and other plants. Plant J **51:** 1126–1136

Palmer AE, Jin C, Reed JC, Tsien RY (2004) Bcl-2-mediated alterations in endoplasmic reticulum Ca^{2+} analyzed with an improved genetically encoded fluorescent sensor. Proc Natl Acad Sci USA **101:** 17404–17409

Palmer AE, Giacomello M, Kortemme T, Hires SA, Lev-Ram V, Baker D, Tsien RY (2006) Ca^{2+} indicators based on computationally redesigned calmodulin-peptide pairs. Chem Biol **13:** 521–530

Palmer AE, Tsien RY (2006) Measuring calcium signaling using genetically targetable fluorescent indicators. Nat Protoc **1:** 1057–1065

Parekh AB, Putney JW Jr (2005) Store-operated calcium channels. Physiol Rev **85:** 757–810

Peiter E (2011) The plant vacuole: emitter and receiver of calcium signals. Cell Calcium **50:** 120–128

Persson S, Harper J (2006) The ER and cell calcium. *In* DG Robinson, ed, The Plant Endoplasmic Reticulum: Plant Cell Monographs. Springer-Verlag, Heidelberg, pp 251–278

Pittman JK, Hirschi KD (2003) Don't shoot the (second) messenger: endomembrane transporters and binding proteins modulate cytosolic Ca^{2+} levels. Curr Opin Plant Biol **6:** 257–262

Qi Z, Stephens NR, Spalding EP (2006) Calcium entry mediated by GLR3.3, an Arabidopsis glutamate receptor with a broad agonist profile. Plant Physiol **142:** 963–971

Ravier MA, Daro D, Roma LP, Jonas JC, Cheng-Xue R, Schuit FC, Gilon P (2011) Mechanisms of control of the free Ca^{2+} concentration in the endoplasmic reticulum of mouse pancreatic β-cells: interplay with cell metabolism and $[Ca^{2+}]_c$ and role of SERCA2b and SERCA3. Diabetes **60:** 2533–2545

Rincón-Zachary M, Teaster ND, Sparks JA, Valster AH, Motes CM, Blancaflor EB (2010) Fluorescence resonance energy transfer-sensitized emission of yellow cameleon 3.60 reveals root zone-specific calcium signatures in Arabidopsis in response to aluminum and other trivalent cations. Plant Physiol **152:** 1442–1458

Rizzuto R, Pozzan T (2006) Microdomains of intracellular Ca^{2+}: molecular determinants and functional consequences. Physiol Rev **86:** 369–408

Sanders D, Pelloux J, Brownlee C, Harper JF (2002) Calcium at the crossroads of signaling. Plant Cell (Suppl) **14:** S401–S417

Sieberer BJ, Chabaud M, Timmers AC, Monin A, Fournier J, Barker DG (2009) A nuclear-targeted cameleon demonstrates intranuclear Ca^{2+}

spiking in *Medicago truncatula* root hairs in response to rhizobial nodulation factors. Plant Physiol **151:** 1197–1206

Spalding EP, Harper JF (2011) The ins and outs of cellular Ca^{2+} transport. Curr Opin Plant Biol **14:** 715–720

Stael S, Wurzinger B, Mair A, Mehlmer N, Vothknecht UC, Teige M (2012) Plant organellar calcium signalling: an emerging field. J Exp Bot **63:** 1525–1542

Sze H, Liang F, Hwang I, Curran AC, Harper JF (2000) Diversity and regulation of plant Ca^{2+} pumps: insights from expression in yeast. Annu Rev Plant Physiol Plant Mol Biol **51:** 433–462

Tanaka K, Swanson SJ, Gilroy S, Stacey G (2010) Extracellular nucleotides elicit cytosolic free calcium oscillations in Arabidopsis. Plant Physiol **154:** 705–719

Vincill ED, Bieck AM, Spalding EP (2012) Ca^{2+} conduction by an amino acid-gated ion channel related to glutamate receptors. Plant Physiol **159:** 40–46

Vincill ED, Clarin AE, Molenda JN, Spalding EP (2013) Interacting glutamate receptor-like proteins in Phloem regulate lateral root initiation in *Arabidopsis*. Plant Cell **25:** 1304–1313

Waadt R, Kudla J (2008) In planta visualization of protein interactions using bimolecular fluorescence complementation (BiFC). Cold Spring Harb Protoc **2008:** pdb.prot4995,

Webb AAR, McAinsh MR, Taylor JE, Hetherington AM (1996) Calcium ions as intracellular second messengers in higher plants. Adv Bot Res **22:** 45–96

Weinl S, Held K, Schlücking K, Steinhorst L, Kuhlgert S, Hippler M, Kudla J (2008) A plastid protein crucial for Ca^{2+}-regulated stomatal responses. New Phytol **179:** 675–686

Wheeler GL, Brownlee C (2008) Ca^{2+} signalling in plants and green algae: changing channels. Trends Plant Sci **13:** 506–514

Winter D, Vinegar B, Nahal H, Ammar R, Wilson GV, Provart NJ (2007) An "Electronic Fluorescent Pictograph" browser for exploring and analyzing large-scale biological data sets. PLoS ONE **2:** e718

Wu Z, Liang F, Hong B, Young JC, Sussman MR, Harper JF, Sze H (2002) An endoplasmic reticulum-bound Ca^{2+}/Mn^{2+} pump, ECA1, supports plant growth and confers tolerance to Mn^{2+} stress. Plant Physiol **130:** 128–137

Yang Y, Costa A, Leonhardt N, Siegel RS, Schroeder JI (2008) Isolation of a strong Arabidopsis guard cell promoter and its potential as a research tool. Plant Methods **4:** 6

Young JJ, Mehta S, Israelsson M, Godoski J, Grill E, Schroeder JI (2006) CO_2 signaling in guard cells: calcium sensitivity response modulation, a Ca^{2+}-independent phase, and CO_2 insensitivity of the *gca2* mutant. Proc Natl Acad Sci USA **103:** 7506–7511